XI International Conference on Computational Plasticity. Fundamentals and Applications
COMPLAS XI
E. Oñate, D.R.J. Owen, D. Peric and B. Suárez (Eds)

ELASTOPLASTIC ANALYSIS OF PLANE STEEL FRAMES UNDER DYNAMIC LOADING

ANDRÉA R.D. SILVA[*], WILLIAM L. FERNANDES[†], RICARDO A.M. SILVEIRA[*] AND PAULO B. GONÇALVES[†]

[*] Department of Civil Engineering, School of Mines, Federal University of Ouro Preto
Campus Universitário s/n, Morro do Cruzeiro, 35400-000 Ouro Preto, MG, Brazil
emails: andreadiassilva@yahoo.com.br, ricardo@em.ufop.br

[†] Department of Civil Engineering, Catholic University (PUC-Rio)
Rua Marquês de São Vicente, 225, Gávea, 22453-900 Rio de Janeiro, RJ, Brazil
emails: wlfernandes13@gmail.com, paulo@puc-rio.br

Key words: Nonlinear Dynamic Behavior, Elastoplastic Analysis, Plastic Hinge Method, Steel Frames, Finite Element Method.

1 INTRODUCTION

Knowledge of structural behavior is essential for designing lighter constructions without affecting their safety and quality standards. Lack of levels and characteristics of dynamic response, for example, can lead to system failure during repetitive loading application, due to the accumulation of structural damage. Thus, it becomes necessary to use more complex theories, such as nonlinear formulations, avoiding simplifications in the process of analysis/design.

Plastic analysis of steel structures enhances several benefits compared to the elastic's, because one of the most important characteristics of this material, the ductility — ability to withstand large deformations before breaking — is fully considered. This allows for force redistribution after the yielding limit of some structural member's cross section has been achieved. This property also promotes the absorption of energy, which becomes extremely important in structures subjected to seismic excitations [1].

Most studies on inelastic analysis rely on the plastic-zone method (or plasticity distributed) or the plastic hinge method (concentrated plasticity or lumped model). The basic difference between them is the refinement degree used to represent the structural member plastification. In the plastic-zone method, the structure is discretized into finite elements and the cross-sections of these elements are subdivided into many fibers. The second-order effects and residual stresses can be considered directly in the analysis. Due to the high degree of refinement, the analyses made with this method are treated as close-to-accurate solutions. However, as it has a high computational cost, the plastic-zone approach is used more for simulation of simple structures that can serve as a calibration for other models and numerical formulations. Few works are found in this line of research directly related to dynamic analysis. Among these are: Kant and Marur [2], Mamaghani et al. [3], and Thai and Kim [4].

In contrast, the plastic hinge approach, which assumes the effects of plasticity concentrated at hinge points located at the ends of the elements, can be classified as an elastic-plastic hinge model or a refined-plastic hinge model. The first one, used in this work, is the simplest way to consider the inelastic effects in structural analysis. The element remains in an elastic regime until the plastic resistance of the cross-section is achieved by forming a plastic hinge. The residual stress effects are not considered. In the refined-plastic hinge model, on the contrary, the process of cross-section plastification can be accompanied and the residual stresses can be considered. By providing an approximate representation of the member behavior in relation to the plastic-zone approach, computationally, the plastic hinge models become significantly less expensive and more applied ([5] – [10]).

The computational system for advanced structural analysis CS-ASA [10] is used in this work. The main characteristic of this computational tool is the accomplishment of the nonlinear static and dynamic analyses of steel plane framed structures. In these analyses, the geometric nonlinearity or second-order effects can be simulated, as well as those introduced by considering semi-rigid connections, and steel inelasticity. The introduction of all these nonlinear effects in the numerical models and formulations makes it possible to establish the stability and strength limit of the structural system in a direct manner, without the necessity to separately verify each member's capacity [11]. For this article, a routine able to simulate the nonlinear cyclic behavior of the material was implemented in the CS-ASA system. Basically, this model is a natural extension of those already implemented in CS-ASA for the static case and can be found in detail in Silva [10]. Therefore, the numerical formulation adopted considers two sources of nonlinearities: the geometric, which includes structural displacement effects, and the physical, caused by the steel's inelasticity. The methods of Newmark (integration process) and Newton-Raphson (iteration process) are used for solving the nonlinear equations of motion. This numerical methodology is discussed throughout the work. Some examples considering the nonlinear inelastic time-history response of planar steel frames will be discussed at the end of the work.

2 FINITE ELEMENT FORMULATION

This section presents the finite element formulation used in the study of the inelastic behavior of steel structures. This formulation, as already highlighted, follows the plastic hinge approach, and the effect of the material yielding is considered in the finite element force-displacement constitutive relationship. Initially, some assumptions should be made. The inelastic behavior is restricted to the ends of the element (nodal points) that will simulate the plastic hinges. The length of these plastic hinges will be null and its deformation is constituted only by inelastic rotation. Once the plastic hinge is formed, the inner forces in cross-section must respect the plastic resistance surface (full yield surface of the section).

Consider then the finite element shown in Figure 1. The beam-column element presented has fictitious section springs attached at its ends. These springs are imagined to have a bending stiffness S_s, which can be defined based on a state parameter ψ (this state parameter monitors the cross-section yielding process and will be discussed in the next subsection). The element force-displacement relationship on the co-rotational local system, considering the cross-section material yielding effect, can be written as [10]:

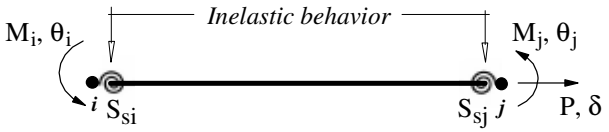

Figure 1: Beam-column finite element with fictitious section springs

$$\begin{Bmatrix} \Delta P \\ \Delta M_i \\ \Delta M_j \end{Bmatrix} = \begin{bmatrix} EA/L & 0 & 0 \\ 0 & S_{si} - S_{si}^2\left(k_{jj} + S_{sj}\right)/\beta & S_{si}S_{sj}k_{ij}/\beta \\ 0 & S_{si}S_{sj}k_{ji}/\beta & S_{sj} - S_{sj}^2\left(k_{ii} + S_{si}\right)/\beta \end{bmatrix} \begin{Bmatrix} \Delta\delta \\ \Delta\theta_i \\ \Delta\theta_j \end{Bmatrix}, \text{ or, } \Delta\mathbf{f}_c = \mathbf{K}_c\Delta\mathbf{u}_c \qquad (1)$$

with $\beta = \left(S_{si} + k_{ii}\right)\left(S_{sj} + k_{jj}\right) - k_{ij}k_{ji}$.

In Eq. (1), the subscribes *i* and *j* are related to the element ends, and the subscript *c* indicates the coordinate system used; *E* is the Young's modulus; *A* is the cross-section area; *L* is the element length; ΔP, ΔM, $\Delta\delta$ and $\Delta\theta$ are, respectively, the axial force, the bending moment, the nodal axial deformation and nodal rotation increments, and are represented in Figure 1. The coefficients of the matrix $\mathbf{K}_c$, besides simulating the section's material plastification at each end of the element, also considers the second-order effects — for relatively large displacements, the lateral deflection of a member can generate additional bending moments because of the presence of axial force. In this case, the terms k_{ii}, k_{jj}, k_{ij} and k_{ji} involved in the simulation are:

$$k_{ii} = k_{jj} = 4EI/L + 2PL/15 + 4PI/(AL) \text{ and } k_{ij} = k_{ji} = 2EI/L - PL/30 + 2PI/(AL) \qquad (2)$$

where *I* represents the moment of inertia.

With the increase of axial force on a section with a plastic hinge already formed, the section resistance may become smaller than the internal forces acting on it. Then, a change in the force-displacement relationship of the element (Eq. 1) will be required so that the section's plastic resistance is not violated. This change can be expressed by the following equation:

$$\begin{Bmatrix} \Delta P \\ \Delta M_i \\ \Delta M_j \end{Bmatrix} = \begin{bmatrix} EA/L & 0 & 0 \\ 0 & C_1K_1 & 0 \\ 0 & 0 & C_2K_2 \end{bmatrix} \begin{Bmatrix} \Delta\delta \\ \Delta\theta_i \\ \Delta\theta_j \end{Bmatrix} + \begin{Bmatrix} 0 \\ \zeta_i \\ \zeta_j \end{Bmatrix}, \text{ or, } \Delta\mathbf{f}_c = \mathbf{K}_{ch}\Delta\mathbf{u}_c + \Delta\mathbf{f}_{ps} \qquad (3)$$

where the parameter vector $\Delta\mathbf{f}_{ps}$ defines the correction of the internal forces. The other matrix $\mathbf{K}_{ch}$ coefficients are presented in Table 1 according to the element end where the plastic hinge is formed. In this table, δM_{pr} is the modification to translate the section moment *M* to the interaction surface (resistance or full yield surface), maintaining the axial force *P* fixed. Details of this change and the process to transform Eqs. (1) and (3) into the global coordinate system, later obtaining the structural system internal forces vector $\mathbf{F}_i$ and stiffness matrix $\mathbf{K}$, can be found in Silva [10].

The section resistance surface adopted here will be presented in the following subsection, which also discusses the numerical procedure used to simulate the material's nonlinear behavior.

Table 1: Parameters in Eq. (3)

Plastic hinge	Parameters			
	C_1	C_2	ζ_1	ζ_2
End *i*	0	1	δM_{pr_i}	$\delta M_{pr_i}(k_{c(3,2)}/k_{c(2,2)})$
End *i*	1	0	$\delta M_{pr_j}(k_{c(2,3)}/k_{c(3,3)})$	δM_{pr_j}
Ends *i* and *j*	0	0	δM_{pr_i}	δM_{pr_j}

$K_1 = k_{c(2,2)} - k_{c(2,3)}k_{c(3,2)}/k_{c(3,3)}$ and $K_2 = k_{c(3,3)} - k_{c(2,3)}k_{c(3,2)}/k_{c(2,2)}$

$k_{c(m,n)}$ is the term corresponding to the row *m* and the column *n* in $\mathbf{K}_c$ (see Eq. 1)

2.1 Cyclic plasticity model

Steel inelasticity is the yielding process of the fibers causing changes in cross-section stress distribution when acting forces increase. Under loading/unloading conditions, the steel can be idealized as an elastic-perfectly plastic material and its constitutive tension-deformation relationship in this case is illustrated graphically in Figure 2a. It is assumed that the plastification occurs when the stress reaches the yield stress σ_y. After that, an increase in loading causes increase in axial deformation without, however, increasing the stress. In this model, the material's permanent deformation appears after the unloading. Load relief makes the material return to the elastic state, remaining, however, with a residual deformation. Models that directly simulate the stress-strain relationship are usually applied in methodologies based on the plastic-zone method. In this work, the cross-section plasticity state, in the same situation, is characterized by the elastic-perfectly plastic model expressed, however, in the moment-curvature relationship as shown in Figure 2b. It is worth clarifying that the potential benefits from the material hardening (strain-hardening) and the Bauschinger effect [6] are ignored in this model.

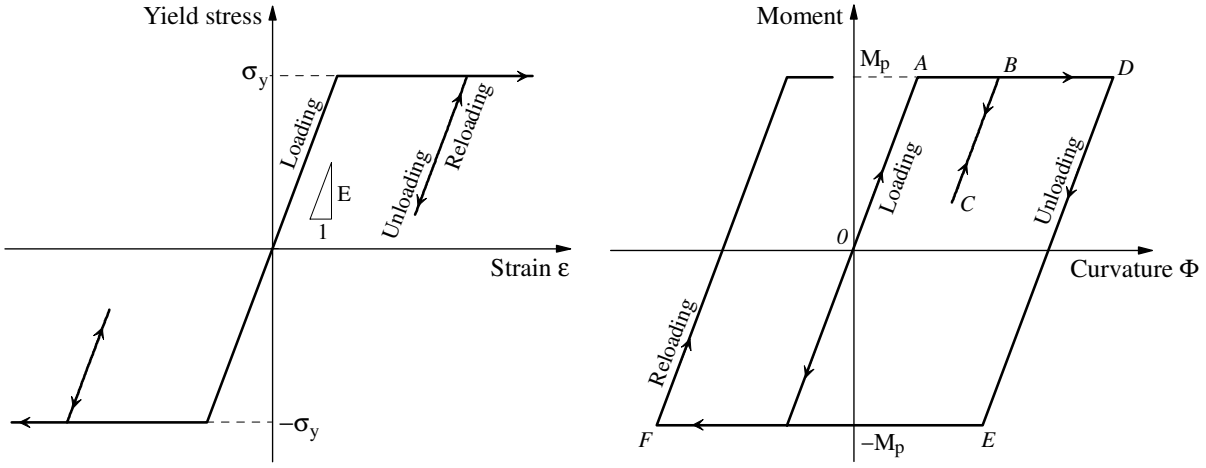

(a) Tension-deformation relation (b) Moment-curvature relation

Figure 2: Elastic-perfectly plastic constitutive material hysteretic model

Figure 2b illustrates the section's behavior during the loading-unloading process through its moment-curvature relationship. The section's material remains elastic along the line *0A*

under loading conditions. When the plastic moment is reached, $M_p = Z\sigma_y$, Z being the module plastic, a plastic hinge is formed and no additional moment can be resisted. So, with the increase in loading, and this section already yielded, the exceeded moment will be redistributed to adjacent members. As a result, the path continues along the horizontal line *AB*. When unloading occurs at *B*, the direction of rotation is reversed and the section returns to the elastic state, but with a residual deformation. In this case, the curve follows the line *BC* parallel to the virgin slope *0A*. If reloaded at point *C*, the path will move along *CB* up to reach again the plastic moment M_p, and continue along the line BD. With the unloading at point *D*, the path *DEF* will be followed where the line *EF* indicates that the negative plastic moment ($-M_p$) has been reached.

The full yield surface, defining the boundary where the material ceases to behave elastically and becomes plastic, will be evaluated from internal acting forces and geometrical characteristics of the finite element cross-section. The structure's resistance limit can be achieved with the development of a plastic mechanism, which is the consequence of a number of plastic hinges formed. If a structural element is subjected to the combined action of bending moment and axial force, its moment capacity M_p is reduced [10]. This influence is seen through the full yield surface defined by equations:

$$M_{pr} = \left[B_f t_f \left(D - t_f \right) + \left((d/2)^2 - \eta^2 \right) t_w \right] \sigma_y \text{, para } \eta \le d/2 \tag{4a}$$

$$M_{pr} = \left[(D/2)^2 - \eta^2 \right] B_f \sigma_y \text{, para } d/2 < \eta \le d/2 + t_f \tag{4b}$$

with:

$$\eta = P / \left(2\sigma_y t_w \right) \text{, para } \eta \le d/2 \tag{5a}$$

$$\eta = \left(P - \sigma_y t_w d \right) / \left(2\sigma_y B_f \right) + d/2 \text{, para } d/2 < \eta \le d/2 + t_f \tag{5b}$$

The interaction equations between the axial force and bending moment follow the requirements of BS 5950 [12] and are valid for the I or H profiles. The full yield surface for the profile W470x74 is exemplified in Figure 3. The axial force and bending moment are parameterized, respectively, by axial yield limit, $P_y = A\sigma_y$, and the plastic moment M_p. Figure 3 shows how the terms B_f, t_f, D, t_w and d are defined, which characterize the profile's web and flange dimensions and appear in Eqs. (4) and (5).

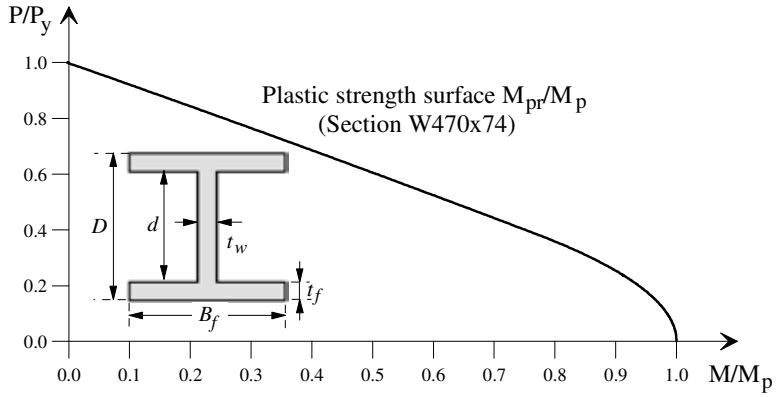

Figure 3: Reduced plastic moment capacity of I-shaped cross-section under axial load

Admitting the material to have elastic-perfectly plastic behavior, it is assumed that a given cross-section remains in elastic regime until its plastic resistance is reached. To accompany the stiffness loss of the cross-section during the loading/unloading process, a dimensionless parameter ψ is adopted. Thus, the development of plasticity in the structure's cross-section members is reflected in the section spring stiffness at the edge of the element, which when using ψ, is defined by equation:

$$S_s = \frac{6EI}{L}\frac{\psi}{1-\psi} \tag{6}$$

It is considered that ψ has the value "1" when the material is in elastic regime, i.e., while the section bending moment does not reach the reduced plastic moment M_{pr}. In this case, using (6), the section remains rigid ($S_s \to \infty$), with the plastic rotation null. On the other hand, with the section yielding ($M = M_{pr}$), ψ reduces to "0" and the section stiffness becomes null ($S_s \to 0$), simulating the plastic hinge formation.

3 SOLUTION PROCEDURE FOR THE TRANSIENT INELASTIC PROBLEM

The equilibrium equation that governs the nonlinear dynamic response of a structural system can be obtained using the Virtual Displacement Principle (VDP). Considering that, besides the restoration tensions provoked by structural deformation and external forces, the structural system is also submitted to inertial and dissipated forces. The equation to obtain the equilibrium of the elements in this system, at time $t + \Delta t$, can be expressed as [13]:

$$\int_{{}^{t}V} \tau_{ij}\delta\varepsilon_{ij}dV + \int_{{}^{t}V} \rho\ddot{d}_k\delta\ddot{d}_k dV + \int_{{}^{t}V} \mu\dot{d}_k\delta\dot{d}_k dV = \delta d_k{}^T f_{ek} \tag{7}$$

where τ_{ij} represents the Cauchy tensor in equilibrium with external excitation f_{ek}; $\delta\varepsilon_{ij}$ are the virtual Green-Lagrange deformation components corresponding to random arbitrary displacements δd_k, which are cinematically compatible with the boundary conditions; ρ is the density or the volumetric mass (mass per volume unit), and μ is the viscous damping coefficient of the material. To determine the equilibrium configuration of the structure in $t + \Delta t$, the updated Lagrangian referential is used. In this case, the configuration in instant t is used as the reference for analysis.

According to the usual finite element procedures, establishing the deformation field and displacement of the elements in function of the nodal displacements and using Eq. (7), it is possible to obtain, in a discretized form, the following matrix equation:

$$\mathbf{M}\ddot{\mathbf{U}} + \mathbf{C}\dot{\mathbf{U}} + \mathbf{F}_i = \lambda(t)\mathbf{F}_r \tag{8}$$

in which $\mathbf{M}$ and $\mathbf{C}$ are the mass and damping matrices, respectively; $\mathbf{U}$, $\dot{\mathbf{U}}$ and $\ddot{\mathbf{U}}$, represent the displacement, velocity and acceleration vectors, respectively, of the structural system; $\mathbf{F}_i$ is the internal force vector; $\mathbf{F}_r$ is the vector that defines the direction of the external excitation; and λ establishes the intensity and direction of the load in a determined instant t.

In a nonlinear structural study, as is done herein, the stiffness matrix should be constantly updated to capture the state of equilibrium influenced by second order effects (P-Δ and P–δ) and inelasticity of the material. Afterwards, it becomes necessary to use an incremental-

iterative solver strategy. For this, a numerical procedure, which combines the methods of Newmark and Newton-Raphson, is used here to obtain a nonlinear dynamic response of the structural system. The computational steps necessary to achieve this objective are detailed in Table 2. Analyzing the numerical procedures adopted, see that the members' plasticity is assessed at the end of each iterative cycle; and the technique described in Section 2 is used for simulating the material nonlinear behavior when the structure is subjected to a cyclic loading. The computational algorithm is summarized in Table 3.

Table 2: Numerical strategy for nonlinear transient analysis

1. Input the material and geometric properties of the frame, and obtain the force vector $\mathbf{F}_r$

2. Start the initial displacement, velocity and acceleration vectors ${}^0\mathbf{U}$, ${}^0\dot{\mathbf{U}}$ and ${}^0\ddot{\mathbf{U}}$

3. Select the time step Δt

4. FOR EACH TIME STEP $t+\Delta t$

4a. Derive the tangent stiffness, mass and damping matrices: **K**, **M**, and **C**

4b. Using Newmark parameters β and γ, calculate the constants:

$a_0 = 1/(\beta\Delta t^2)$; $a_1 = \gamma/(\beta\Delta t)$; $a_2 = 1/(\beta\Delta t)$; $a_3 = 1/(2\beta)-1$; $a_4 = \gamma/\beta-1$;

$a_5 = \Delta t\left(\gamma/(2\beta)-1\right)$; $a_6 = a_0$; $a_7 = -a_2$; $a_8 = -a_3$; $a_9 = \Delta t(1-\gamma)$; $a_{10} = \alpha\Delta t$

4c. Form the effective stiffness matrix: $\hat{\mathbf{K}} = \mathbf{K} + a_0\mathbf{M} + a_1\mathbf{C}$

4d. Calculate: $\hat{\mathbf{F}} = {}^{(t+\Delta t)}\lambda\mathbf{F}_r + \mathbf{M}\left(a_2\,{}^t\dot{\mathbf{U}} + a_3\,{}^t\ddot{\mathbf{U}}\right) + \mathbf{C}\left(a_4\,{}^t\dot{\mathbf{U}} + a_5\,{}^t\ddot{\mathbf{U}}\right) - {}^t\mathbf{F}_i$

4e. Solve for displacement increments: $\hat{\mathbf{K}}\Delta\mathbf{U}^0 = \hat{\mathbf{F}}$

5. NEWTON-RAPHSON ITERATION: k = 1, 2, 3,...

5a. Evaluate the approximation of the acceleration, velocities and displacements:

${}^{(t+\Delta t)}\ddot{\mathbf{U}}^{(k-1)} = a_0\Delta\mathbf{U}^{(k-1)} - a_2\,{}^t\dot{\mathbf{U}} - a_3\,{}^t\ddot{\mathbf{U}}$, ${}^{(t+\Delta t)}\dot{\mathbf{U}}^{(k-1)} = a_1\Delta\mathbf{U}^{(k-1)} - a_4\,{}^t\dot{\mathbf{U}} - a_5\,{}^t\ddot{\mathbf{U}}$, and

${}^{(t+\Delta t)}\mathbf{U}^k = {}^t\mathbf{U} + \Delta\mathbf{U}^{(k-1)}$

5b. Update the geometry of the frame

5c. Evaluate the internal forces vector: ${}^{(t+\Delta t)}\mathbf{F}_i^{(k-1)} = {}^t\mathbf{F}_i + \mathbf{K}\Delta\mathbf{U}^{(k-1)}$

5d. Form: ${}^{(t+\Delta t)}\mathbf{R}^k = {}^{(t+\Delta t)}\lambda\mathbf{F}_r - \left(\mathbf{M}\,{}^{(t+\Delta t)}\ddot{\mathbf{U}}^{(k-1)} + \mathbf{C}\,{}^{(t+\Delta t)}\dot{\mathbf{U}}^{(k-1)} + {}^{(t+\Delta t)}\mathbf{F}_i^{(k-1)} - {}^{(t+\Delta t)}\mathbf{F}_{ps}^{(k-1)}\right)$

5e. Solve for the corrected displacement increments $\hat{\mathbf{K}}\delta\mathbf{U}^k = {}^{(t+\Delta t)}\mathbf{R}^k$

5f. Evaluate the corrected displacement increments: $\Delta\mathbf{U}^k = \Delta\mathbf{U}^{(k-1)} + \delta\mathbf{U}^k$

5g. Check the convergence of the iteration process:

$\|\Delta\mathbf{U}^k\| / \|{}^t\mathbf{U} + \Delta\mathbf{U}^k\| \le \xi$, where ξ is a tolerance factor **NO**: Go to 5

5h. Calculate the acceleration, velocities and displacements at time $t+\Delta t$

${}^{(t+\Delta t)}\ddot{\mathbf{U}}^k = a_0\Delta\mathbf{U}^k - a_2\,{}^t\dot{\mathbf{U}} - a_3\,{}^t\ddot{\mathbf{U}}$, ${}^{(t+\Delta t)}\dot{\mathbf{U}}^k = a_1\Delta\mathbf{U}^k - a_4\,{}^t\dot{\mathbf{U}} - a_5\,{}^t\ddot{\mathbf{U}}$ and

${}^{(t+\Delta t)}\mathbf{U}^k = {}^t\mathbf{U} + \Delta\mathbf{U}^k$

6. FOR THE NEXT TIME STEP

6a. Evaluate the internal forces vector: ${}^{(t+\Delta t)}\mathbf{F}_i = {}^t\mathbf{F}_i + \mathbf{K}\Delta\mathbf{U}^k$

6b. Evaluate the plastification at the ends of the finite elements (see Table 4)

Table 3: Algorithm for modeling of section behavior under cyclic loading

1. Consider the internal forces vectors ${}^{(t+\Delta t)}\mathbf{F}_i$ and ${}^{t}\mathbf{F}_i$

2. FOR EACH FINITE ELEMENT

3. FOR EACH NODAL POINT OF THE ELEMENT

4. Consider the moments ${}^{(t+\Delta t)}M$ and ${}^{t}M$, and the axial force ${}^{(t+\Delta t)}P$ at section

5. Evaluate the incremental moment in this section: $\Delta M = {}^{(t+\Delta t)}M - {}^{t}M$

6. Consider the reduced plastic yield moment M_{pr} (see Eq. 4)

7. If $(M \cdot \Delta M \geq 0)$ then ⇨ LOADING CONDITION

If $(|M| < |M_{pr}|)$: $\psi = 1$ and $S_s = 10^{10}\ EI/L$ (rigid section – elastic behavior)

If $(|M| \geq |M_{pr}|)$: $\psi = 0$ and $S_s = 10^{-10}\ EI/L$ (plastic hinge – plastic behavior)

8. If $(M \cdot \Delta M < 0)$ then ⇨ UNLOADING CONDITION

$\psi = 1$ and $S_s = 10^{10}\ EI/L$ (rigid section – elastic behavior)

9. Go to step 4 in Table 2

4 NUMERICAL APPLICATIONS

In this section, the methodology presented for nonlinear dynamic analysis is used to obtain the response of three planar structural systems with elastic-perfectly plastic material. All structures were also investigated by Chan and Chui [6] and their results are used for validation of the numerical strategy proposed. No viscous damping was considered and time increments of 10^{-3}s were adopted in the numerical integration process.

4.1 Toridis-Khozeimeh portal frame

The simple portal frame with fixed ends shown in Figure 4, initially studied by Toridis and Khozeimeh [14] and subsequently by Marur and Kant [2], is the first example of this section. The steel profile masses of the structure members were multiplied by 625 and considered concentrated in the elements nodal points following the modeling made by the aforementioned authors. Three finite elements were used in the modeling of each of the three structural members.

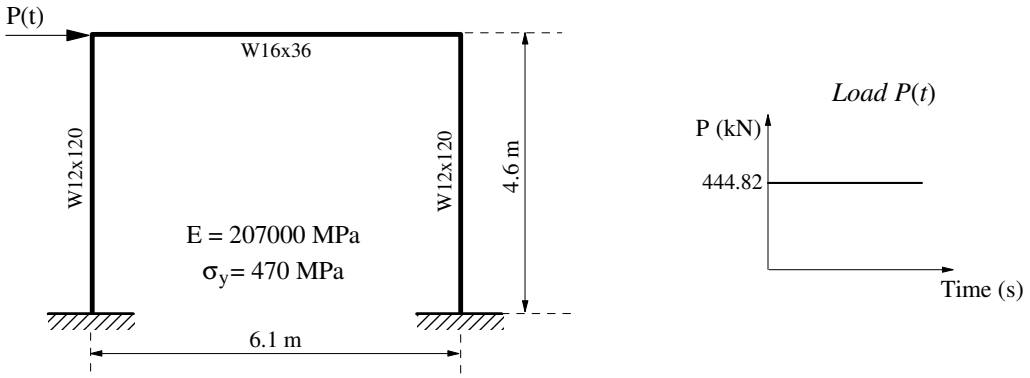

Figure 4: Toridis-Khozeimeh portal frame: geometry and loading

A constant impact load equal to 444.82 kN is applied on top of the column on the left side of the frame, and the transient responses of this structure are presented in Figure 5. Figure 5a shows the horizontal displacement time-history at the point of application of the load for the perfectly elastic material; and Figure 5b presents the dynamic response considering the elastic-perfectly plastic material. Figure 5a also indicates the displacement obtained from the static elastic analysis, u = 3.97 cm, which represents half of the maximum amplitude obtained in dynamic analysis. Comparing the displacement time-histories for these studies, according to Figure 5b, it can be seen that the amplitudes begin diverting more significantly from 0.55s, due to the increase of plastic deformations. There is, moreover, a constant movement response. In this case, the material exhibits an elastic behavior but with a residual deformation. This is a feature of elastic-perfectly plastic model used on this work, and just as in the elastic model, it does not allow the dissipation of energy.

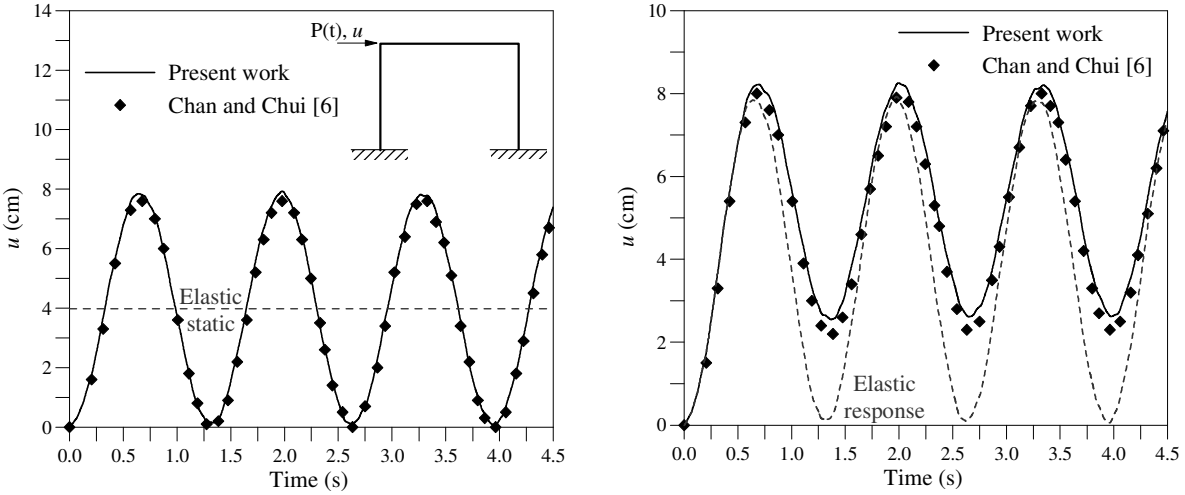

(a) Elastic response (b) Elastoplastic response

Figure 5: Time history of the horizontal displacement, u, on top of the frame

4.2 Steel arch-shaped frame

The structure shown in Figure 6 is now studied. The curved shape of this structure was obtained modeling it with six pieces of steel profile UB305x165x40 kg/m. Besides Chan and Chui [6], Lee et al. [5] also investigated the transient elastic-perfectly plastic response of the arch but using a bilinear plastic resistance surface.

Six finite elements, each modeling of the steel parts, were adopted on discretization. The steel arch, which has fixed supports, is subjected to an vertical impact load $P(t)$ applied at its top (the triangular decaying over time of this vertical load is showed in Figure 6). Gravitational loads of intensity 10 kN statically applied and a lumped mass of 0.5 kNs^2/m attached to each node were also considered. The time histories of the vertical deflection at the arch top are illustrated in Figure 7. A permanent plastic deformation is observed, and the amplitude of displacement becomes virtually constant indicating that the structure remains in the elastic regime after 0.012s.

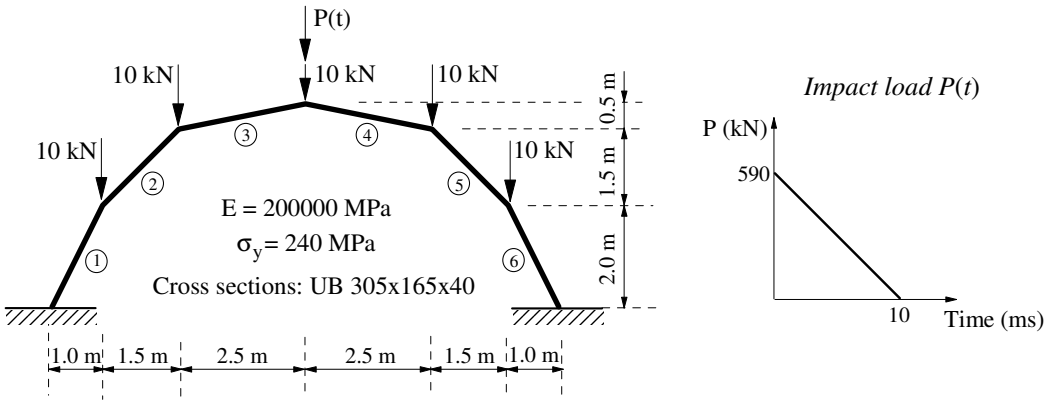

Figure 6: Arch-shaped frame: geometry and loading

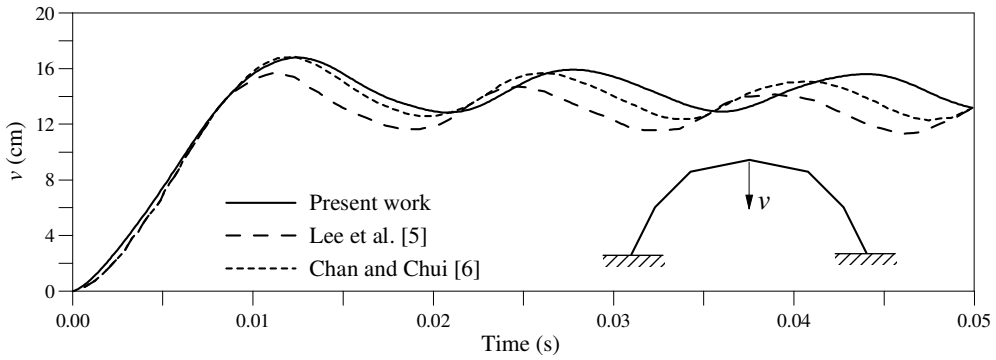

Figure 7: Dynamic elastoplastic response of the arch under impact load

4.3 Simple portal frame with initial geometric imperfection

In the last analysis, attention is given to the yield stress effect on the structural response of a simple portal frame with pinned supports illustrated in Figure 8. An initial geometric imperfection Δ_0 in columns was assumed. To predict a more realistic behavior of this structure, two heavy gravitational loads of 200 kN acting at the ends of the beam (or at the top of the columns) were considered. These loads induce axial forces in columns, and as a consequence, additional bending moments appear, reducing the stiffness of these members and structural system (P-Delta effect in the analysis). The beam and columns of the frame are made by hot-rolled steel profiles W8x48.

The nonlinear transient frame responses considering the elastic and inelastic (elastoplastic) material behavior are illustrated in Figure 8. Yield stress equal to 235 MPa and 260 MPa were adopted in the elastoplastic analysis. Figure 8b shows the members' sections plastic resistance surface considered. In Figures 8c and 8d can be observed that the magnitude of plastic deformation decreases with the increasing of the material yield stress. In the limit, i.e., for $\sigma_y \to \infty$, the material would tend to present the elastic behavior, whose results are plotted in Figure 8a.

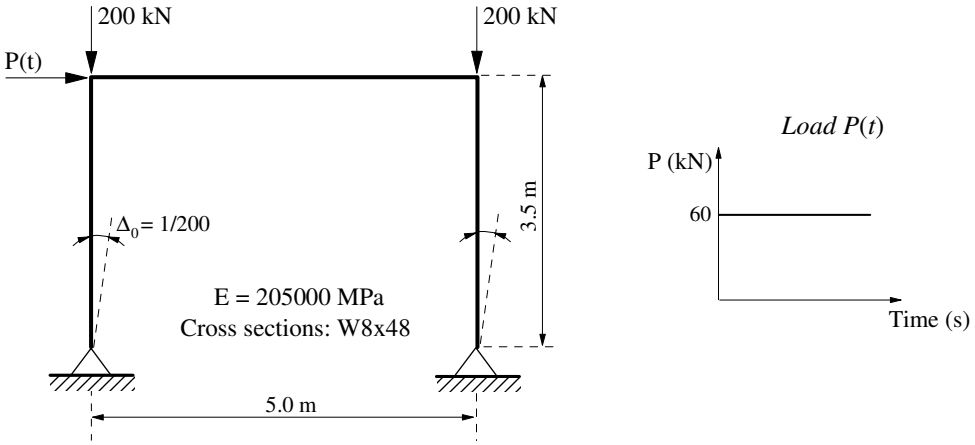

Figure 8: Simple portal frame with initial geometric imperfection: geometry and loading pattern

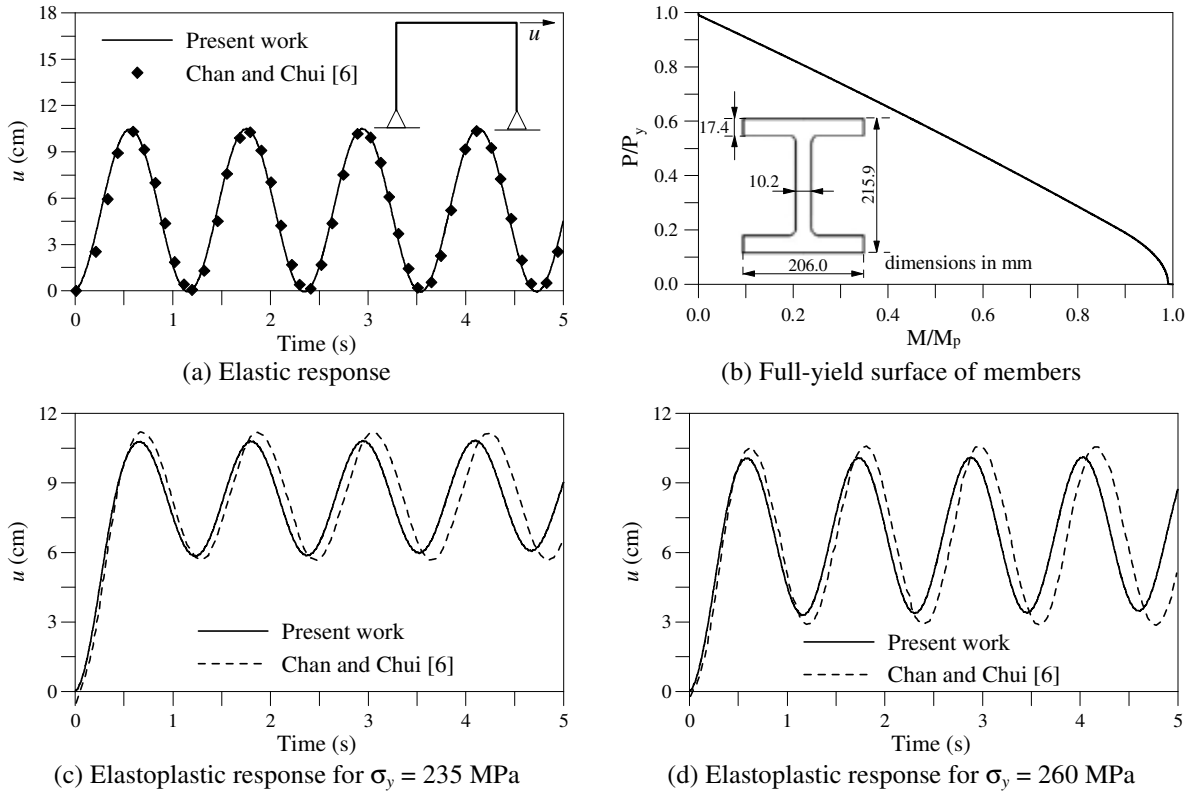

(a) Elastic response

(b) Full-yield surface of members

(c) Elastoplastic response for σ_y = 235 MPa

(d) Elastoplastic response for σ_y = 260 MPa

Figure 9: Dynamic elastic and inelastic responses of the simple portal frame

5 FINAL REMARKS AND FUTURE RESEARCH

This article described a numerical methodology for nonlinear dynamic analysis of steel frames. The main feature of the finite element formulation adopted is the consideration of the geometric nonlinear effects and the material elastic-perfectly plastic behavior. The plastic hinge model was used to evaluate the members' section yielding. The steel section gradual yielding and residual stresses were not considered. Numerical examples presented

demonstrated the applicability of the numerical strategy proposed, and the good agreement between the results here obtained and those found in literature have validated such strategy.

It is worth informing that future authors' research should address the influence of the combined effects of geometric nonlinearity, steel inelasticity and semi-rigid connections on the nonlinear static and dynamic behavior of steel structures. In these studies, the refined plastic hinge model (with steel section gradual yielding), which enables the energy dissipation through the plastic hinges, will be adopted.

ACKNOWLEDGMENTS

The authors are grateful to CAPES, CNPq and FAPEMIG for the financial supports received for this research.

REFERENCES

[1] Lui, E.M. *Structural Steel Design*. In Structural Engineering Handbook, Ed. W.F. Chen, CRC Press LLC, (1999).

[2] Marur, S.R. and Kant, T. A stress correction procedure for the analysis of inelastic frames under transient dynamic loads. *Computers & Structures* (1994) **50**(5) 603-613.

[3] Mamaghani, I. H.P., Usami T. and Mizuno E. Inelastic large structural steel cyclic loading. *Engineering Structures* (1996) **18**(9) 659-668.

[4] Thai, H.-T. and Kim, S.-E. Second-order inelastic dynamic analysis of steel frames using fiber hinge method. *Journal of Constr. Steel Re* (2011) doi:10.1016/j.jcsr.2011.03.022.

[5] Lee, S.L., Swaddiwudhipong, S. and Alwis, W.A.M. Elasto-plastic dynamic analysis of plane frames and deep arches. *Computational Mechanics* (1988) **3** 39-48.

[6] Chan, S.L. and Chui, P.P.T. *Non-linear Static and Cyclic Analysis of Steel Frames with Semi-Rigid Connections*. Elsevier, Oxford, (2000).

[7] Kim, S.-E., Cuong N.-H. and Lee D.-H. Second-order inelastic dynamic analysis of 3-D steel frames. *International Journal of Solids and Structures* (2006) **43**: 1693–1709.

[8] Au, F.T.K. and Yan Z.H. Dynamic analysis of frames with material and geometric nonlinearities based on the semirigid technique. *International Journal of Structural Stability and Dynamics* (2008) **8**(3): 415–438.

[9] Sekulovic, M. and Nefovska-Danilovic, M. Contribution to transient analysis of inelastic steel frames with semi-rigid connections. *Engineering Structures* (2008) **30**: 976–989.

[10] Silva, A.R.D. *Computational System for Static and Dynamic Advanced Analysis of Steel Frames,* D.Sc. Dissertation, PROPEC/Deciv/UFOP, Ouro Preto/MG, Brazil, (2009) (in Portuguese).

[11] Chen, W.F and Toma, S. *Advanced Analysis of Steel Frames*, CRC Press, Boca Raton, Flórida, (1994).

[12] BS 5950. *Structural Use of Steelwork in Buildings. Part 1*. British Standards Institution, London, England, (1990).

[13] Zienkiewicz, O.C. and Taylor, R.L. *The finite element method*. McGraw Hill, Vol. I., (1989), Vol. II, (1991).

[14] Toridis, T.G. and Khozeimeh, K. Inelastic response of frames to dynamic loads. *Journal of Engineering Mechanics* (1971) **97**(3), 847-863.